8. M. J. Kiel, O. H. Yilmaz, T. Iwashita, C. Terhorst, S. J. Morrison, *Cell* **121**, 1109 (2005).
9. D. A. Sipkins *et al.*, *Nature* **435**, 969 (2005).
10. Materials and methods are available as supporting material on *Science* Online.
11. A. Peled *et al.*, *Science* **283**, 845 (1999).
12. T. Lapidot, O. Kollet, *Leukemia* **16**, 1992 (2002).
13. H. E. Broxmeyer, *Curr. Opin. Hematol.* **15**, 49 (2008).
14. D. J. Ceradini *et al.*, *Nat. Med.* **10**, 858 (2004).
15. C. Hitchon *et al.*, *Arthritis Rheum.* **46**, 2587 (2002).
16. B. Nervi, D. C. Link, J. F. DiPersio, *J. Cell. Biochem.* **99**, 690 (2006).
17. G. Calandra *et al.*, *Bone Marrow Transplant.* **41**, 331 (2008).
18. W. Bensinger *et al.*, *J. Clin. Oncol.* **13**, 2547 (1995).
19. N. Okumura *et al.*, *Blood* **87**, 4100 (1996).
20. R. L. Driessen, H. M. Johnston, S. K. Nilsson, *Exp. Hematol.* **31**, 1284 (2003).
21. L. K. Ashman, *Int. J. Biochem. Cell Biol.* **31**, 1037 (1999).
22. S. Sharma *et al.*, *Stem Cells Dev.* **15**, 755 (2006).
23. N. Théou-Anton *et al.*, *Br. J. Cancer* **94**, 1180 (2006).
24. K. A. Giehl, U. Nagele, M. Vokenandt, C. Berking, *J. Cutan. Pathol.* **34**, 7 (2007).
25. G. Bellone *et al.*, *Int. J. Oncol.* **29**, 851 (2006).
26. M. Tao *et al.*, *Cytokine* **12**, 699 (2000).
27. R. Zheng, K. Klang, N. C. Gorin, D. Small, *Leuk. Res.* **28**, 121 (2004).

28. We thank A. Chenn, K. Cohen, L. Godley, and R. Salgia for critical discussions and reading of the manuscript; A. Chenn for assistance with retroviral cell transduction; A. Wickrema for help with CD34$^+$ purification; V. Bindokas for imaging expertise; and S. Gurbuxani for assistance with histopathology interpretation. Supported by a grant from the Illinois Regenerative Medicine Institute (IRMI), an NIH (National Cancer Institute) K08 award (5K08CA112126-02), and an NIH Director's DP2 award (1DP2OD002160-01). A patent application related to this work has been filed by the University of Chicago.

Supporting Online Material

www.sciencemag.org/cgi/content/full/322/5909/1861/DC1
Materials and Methods
Figs. S1 to S13
Movies S1 and S2

7 August 2008; accepted 19 November 2008
10.1126/science.1164390

Representation of Geometric Borders in the Entorhinal Cortex

Trygve Solstad, Charlotte N. Boccara,* Emilio Kropff,* May-Britt Moser, Edvard I. Moser†

We report the existence of an entorhinal cell type that fires when an animal is close to the borders of the proximal environment. The orientation-specific edge-apposing activity of these "border cells" is maintained when the environment is stretched and during testing in enclosures of different size and shape in different rooms. Border cells are relatively sparse, making up less than 10% of the local cell population, but can be found in all layers of the medial entorhinal cortex as well as the adjacent parasubiculum, often intermingled with head-direction cells and grid cells. Border cells may be instrumental in planning trajectories and anchoring grid fields and place fields to a geometric reference frame.

An animal's current position in the environment is encoded by a network of hippocampal and parahippocampal neurons with diverse spatial firing properties. Within this network, at least three cell types contribute to the computation of self-location: place cells, which fire when the animal moves through a particular location in space (*1*–*3*); head-direction cells, which fire when the animal is facing in a certain direction (*4*–*7*); and grid cells, whose multiple sharply localized firing fields form a remarkably regular triangular pattern across the environment (*3*, *7*–*9*). In addition to these cell types, computational models posit the existence of cortical "boundary vector cells," whose activity patterns encode the animal's distance from salient geometric borders (*10*, *11*). Based on predictions from these models, we investigated whether proximity to borders is represented by specific cell types in the entorhinal spatial representation circuit (*12*).

A total of 624 principal cells were recorded from the dorsocaudal quarter of the medial entorhinal cortex (MEC) and adjacent parasubiculum in 13 rats (fig. S1). Neural activity was sampled while these animals foraged in enclosures with moveable walls and barriers. The animals were first tested in a square enclosure (1 m by 1 m or 1.5 m by 1.5 m) with 50-cm-high walls. Many recorded cells were grid cells and head-direction cells (*7*–*9*), but in addition the data included a previously unknown class of entorhinal cells that fired exclusively along one or several walls of the enclosure (Fig. 1 and fig. S2). These cells were identified by computing, for each cell, the difference between the maximal length of a wall touching upon a single firing field and the average distance of the fields from the nearest wall, divided by the sum of those values (*12*). Border scores ranged from –1 for cells with central firing fields to +1 for cells with fields that perfectly lined up along at least one entire wall. "Border cells" were defined as spatially stable cells with border scores above 0.5. A total of 69 cells from 12 animals passed this criterion (Fig. 1 and fig. S2) (*13*). In these cells, 86.0 ± 0.6% of the spikes occurred closer to the walls than to the center of the box per unit of time [mean ± SEM; $t(68) = 17.4$, one-sample t test, $P < 0.001$; expected value 75%]. Only 3.6 ± 1.0% of the

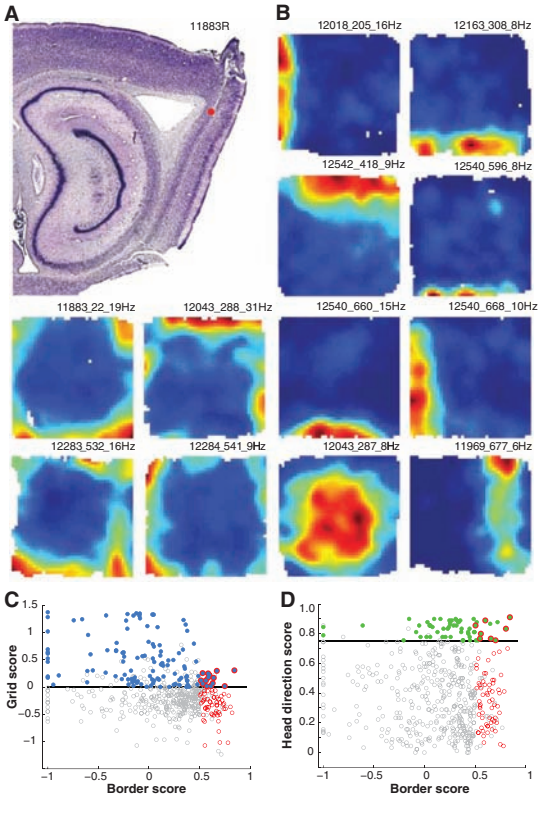

Fig. 1. Examples of border cells in the MEC and adjacent parasubiculum. (**A**) Sagittal Nissl-stained section showing a representative recording location in the MEC (red dot, recording location; rat number and hemisphere (R, right) are indicated; see fig. S1 for all other recording positions). (**B**) Color-coded rate maps for 12 border cells. Red is maximum, dark blue is zero. Pixels not covered are white. Animal numbers (five digits), cell numbers (two or three digits), and peak firing rates are indicated above each panel. Cells 287 and 677 did not pass the criterion for border cells because the fields were located at some distance from the wall; the number of such cells was fewer than 10. See fig. S2 for the complete set of rate maps, trajectories, and directional tuning curves, and representative waveforms and tetrode clusters. (**C** and **D**) Scatter plots showing correlation between border scores and grid scores (C) or head-direction scores (D) (*12*). Each dot in the scatter plot corresponds to one cell (red, border cells; blue, grid cells; green, head-direction cells; gray, cells not passing any criterion, including cells with high spatial or directional scores but low stability; double-colored dots, cells that satisfy criteria for two cell classes). Horizontal lines indicate thresholds for grid and head-direction cells.

Kavli Institute for Systems Neuroscience and Centre for the Biology of Memory, Norwegian University of Science and Technology, 7489 Trondheim, Norway.

*These authors contributed equally to this work.
†To whom correspondence should be addressed. E-mail: edvard.moser@ntnu.no

central area was part of a firing field [expected value 25%; $t(68) = 22.1$, $P < 0.001$]. Fifty-two of the cells fired along a single wall; the remaining 17, mostly from the deep layers of the MEC, had fields along two, three, or four walls (fig. S2A). On average, the border field along the dominant wall covered 75.4 ± 1.8% of the length of the wall. The mean distance between the active bins in the field and the wall was 8.4 ± 0.3% of the box length. An additional set of fewer than 10 cells, excluded by the formal criterion, had fields that were parallel to the box walls but separated by a stripe of inactivity between the walls and the field (Fig. 1B, cells 287 and 677). The activity pattern of the border cells was fundamentally different from that of grid cells and head-direction cells recorded simultaneously on the same tetrodes [Fig. 1, C and D, and supporting online material (SOM) text]. Border cells were found in all layers of the MEC and in the adjacent parasubiculum (fig. S1 and SOM text). Thirty-one of 69 border cells were modulated by the theta rhythm (fig. S3).

If the activity was determined by the walls rather than other localized variables, the cells should continue to fire along their preferred walls after changes in the length of the box, and the mean firing distance from the nearest wall might remain unchanged. This prediction was confirmed for most of the cells that were classified as border cells in the small square enclosure. Extending the 1-m–by–1-m square to a 1-m–by–2-m or 2-m–by–1-m rectangle caused a corresponding extension of the firing field if the field was parallel to the extended wall but not if its long axis was orthogonal to the direction of extension (44 cells; Fig. 2A and fig. S4). The fraction of spikes along the walls per unit of time was not changed [79.9 ± 1.7% in the square and 80.8 ± 1.5% in the rectangles; paired t test, $t(43) = 0.45$]. The proportion of the central area covered by firing fields [5.0 ± 1.0% in the square and 7.9 ± 1.5% in the rectangle; paired t test, $t(43) = 2.3$, $P < 0.05$] remained far below the chance level of 25% [for the rectangle, $t(43) = 11.8$, < 0.001], suggesting that the firing was indeed controlled by the walls of the environment.

Do border cells primarily encode the periphery of the environment or are they tuned to barriers more generally, irrespective of their continuity with the other borders? We recorded the activity of 22 border cells after inserting a discrete wall into the square enclosure (*11*, *12*) (Fig. 2B and figs. S5 and S6). Only cells with fields along a single wall were analyzed (12 cells). When the wall was inserted in parallel with the original firing field, an additional field emerged in the rate map of all cells, although only 9 of the new fields met our selection criteria for quantitative analysis. In all 12 cases, the new field lined up along the inserted wall. The new field and the parent field were always on the same side of the insert relative to the distal room cues (for example, both were on the east side in Fig. 2B). The new field covered 68.7 ± 8.2% of the inserted wall on this side. The coverage of the opposite side (the side that faced the parent field) was 0 in all cases. Reducing the height of the barrier from 50 cm to 5 cm did not abolish the new field as long as the animal's trajectory was impeded (fig. S6; three experiments).

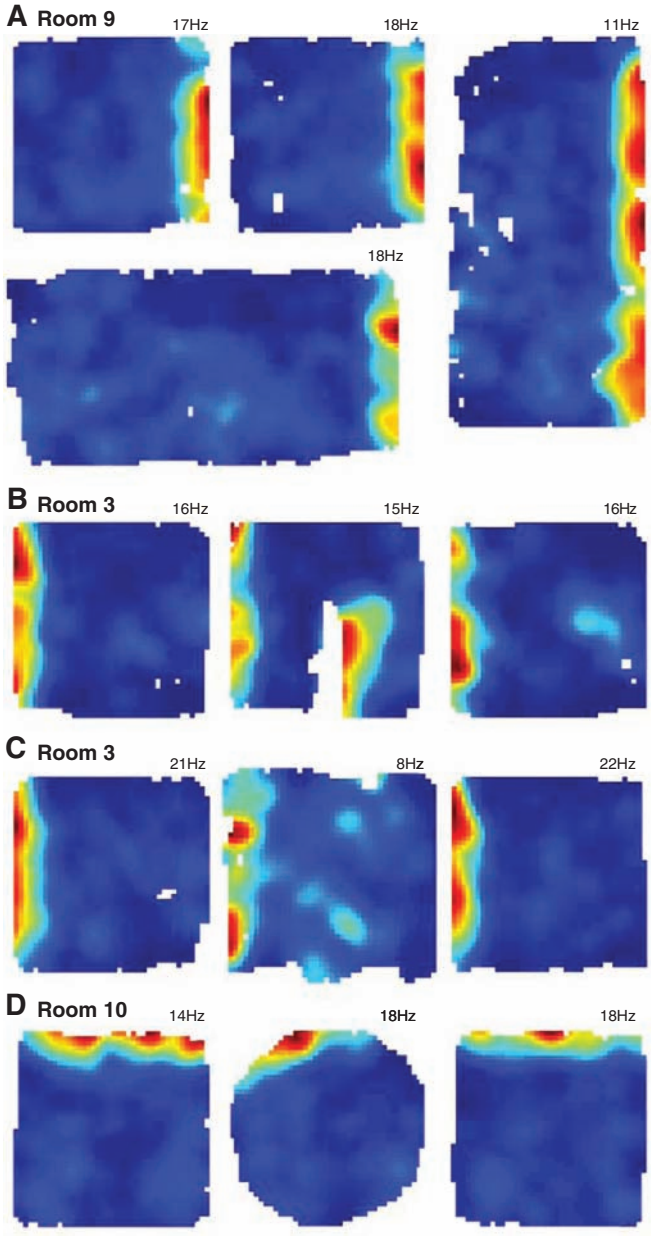

Fig. 2. Border cells express proximity to boundaries in a number of environmental configurations. (**A** to **D**) Color-coded rate maps for a representative border cell in boxes with different geometric configurations (cell 205 of rat 12018). Each panel shows one trial. Symbols are as in Fig. 1B. (A) The border field follows the walls when the square enclosure is stretched to a rectangle. (B) Introducing a discrete wall (white pixels) inside the square causes a new border field to appear (middle panel). The new field has the same orientation relative to distal cues as the original field on the peripheral wall. (C) Border fields persist after removal of the box walls (middle panel). Without walls, the drop along the edges was 60 cm. (D) Preserved firing along borders across rooms and geometrical shapes. All trials in (D) were recorded in a different room than those in (A) to (C). The conditions favor hippocampal global remapping between rooms and rate remapping within rooms (*12*, *16*, *22*) (fig. S9).

To determine whether border cells also respond to boundaries other than walls, the box walls were removed and the animals were tested on the remaining open surface, which now had a 60-cm drop on all four sides. In general, border fields could still be identified (Fig. 2C and figs. S7 and S8). The fraction of spikes along the walls per unit of time was not changed significantly [84.4 ± 1.5% with walls, 80.3 ± 3.1% without walls, $t(9) = 1.8$, $P > 0.10$], although the fraction of the central area that was part of a firing field increased [2.8 ± 2.1% with walls, 11.2 ± 4.1 without walls, $t(9) = 2.5$, $P < 0.05$; expected value 25%, $t(9) = 3.3$, $P < 0.01$]. The persistence of activity along the edges suggests that the cells respond to a variety of borders.

Unlike place cells (*14*, *15*), grid cells and head-direction cells retain their basic activity pattern across environments (*5*, *9*, *16*, *17*). To determine whether border cells are similarly context-independent, we first compared the activity of 27 cells in two different rooms, using square recording boxes in each room. The fraction of spikes along the walls, normalized by dwell times, did not change between the rooms [83.0 ± 1.5% versus 84.7 ± 1.3%; paired t test, $t(26) = 1.41$, $P > 0.15$; Fig. 2, B and C, versus D], nor did the proportion of the central area that was part of a firing field [11.5 ± 4.1% versus 7.5 ± 2.8%; $t(26) = 0.98$, $P > 0.30$]. We also compared the firing patterns of 21 border cells in two differently shaped enclosures, a square and a circle,

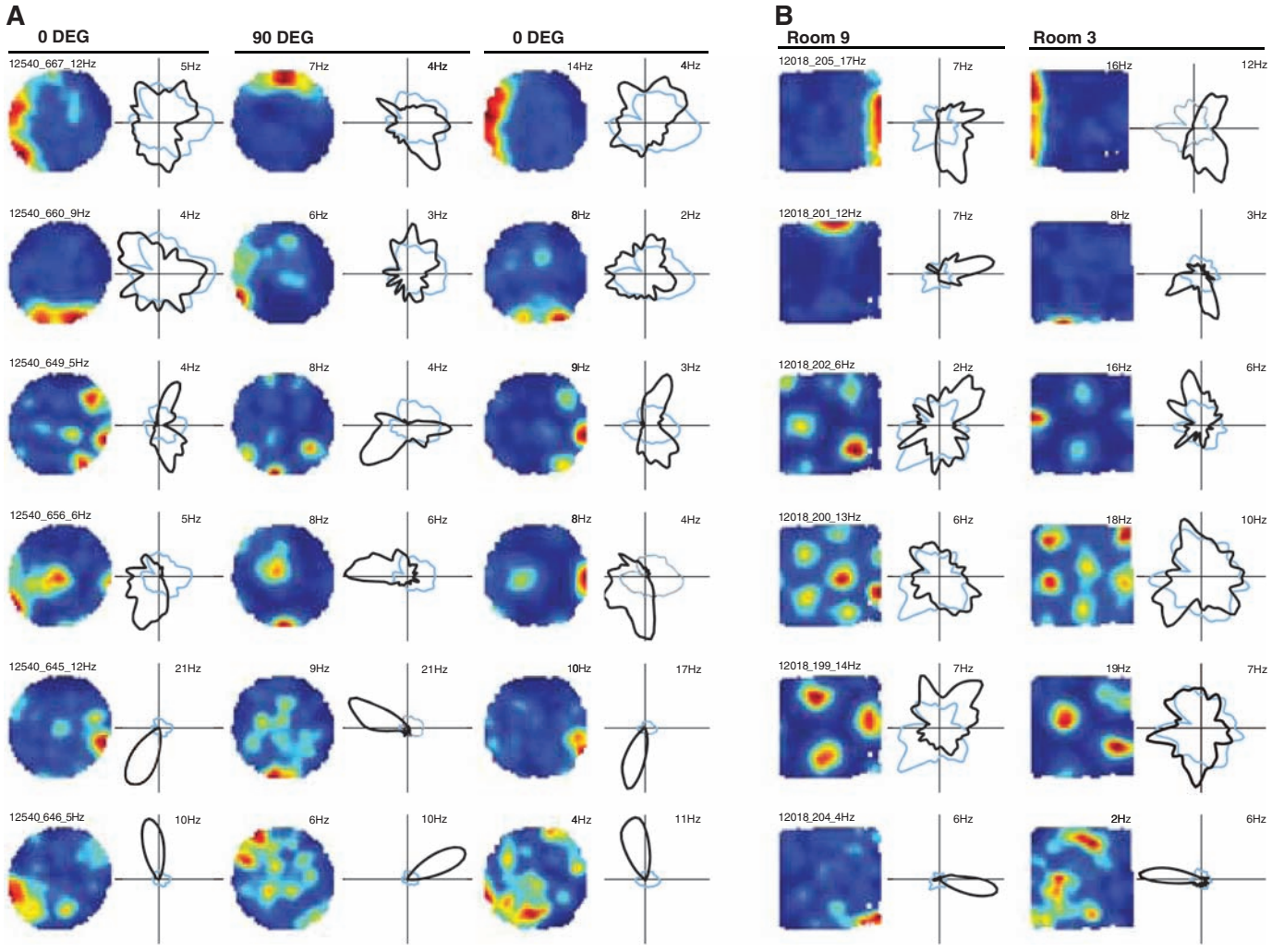

Fig. 3. Border cells, grid cells, and head-direction cells respond coherently to environmental manipulations. (**A**) Rate and head-direction maps for two border cells (top two rows), two grid cells with some head-directional modulation (middle two rows), and two head-direction cells (bottom two rows) recorded simultaneously before and after the rotation of a polarizing cue card (left and right columns, 0°; middle column, 90°). The polar plots show firing rate as a function of head direction (black traces) and the time that the rat faced each direction (blue traces). Peak firing rate is indicated. (**B**) Rate maps and polar plots for two border cells (top two rows), three grid cells (middle three rows), and one head-direction cell (bottom row) in two different rooms. The cells were recorded simultaneously.

in a single room (Fig. 2D and fig. S9). Again, the time-normalized fraction of spikes along the walls was not different [square, 87.1 ± 1.0%; circle, 85.0 ± 1.6%; paired t test, $t(20) = 1.67$, $P > 0.10$; Fig. 2D] and the firing fields covered a similar proportion of the central area of the environments [6.1 ± 2.2% and 12.7 ± 4.3; $t(20) = 1.95$, $P > 0.05$]. The persistence of border-related activity across environments, under conditions that often lead to realignment in grid cells and remapping in place cells (*16*) (fig. S8), suggests that the firing of these cells is primarily defined by geometric borders and less by the content of the environment or the training history of the animal.

Does the representation of borders, grid positions, and directions remain coherent across environments? We recorded 10 border cells along with grid cells and head-direction cells in five experiments. When the cue card on the wall of the circle was rotated 90°, simultaneously recorded border cells always rotated in concert (three experiments; pairwise difference in rotation 1°, 1°, and 9°; Fig. 3A). The same was observed with simultaneously recorded border cells and grid cells (mean difference between cell types 0°, 7.2°, and 9.5°; Fig. 3A) and with simultaneously recorded border cells and head-direction cells (mean difference 8.5°, 12.5°, and 13.6°; Fig. 3A; two of these experiments also included grid cells). When the animals were tested in different rooms, differences in the relative orientation of simultaneously recorded border cells were retained; that is, cells with fields on opposite walls in one room also fired along opposite walls in the other room, and their relation to grid cells and head-direction cells remained constant (Fig. 3B).

Taken together, these findings provide evidence for a previously unknown cell type in the spatial representation circuit of the MEC. Border cells have firing fields that line up along selected geometric borders of the proximal environment, irrespective of their length and continuity with other borders. The observation of border cells across all layers of the MEC confirms predictions from computational models that posit the existence of a boundary-responsive cortical cell population upstream of the hippocampus (*10*, *11*, *18*). Given that border cells are distributed widely in the circuit, information about obstacles and borders should be accessible to the majority of the entorhinal grid cells as well as to external target regions involved in path planning (*19*). By defining the perimeter of the environment, border cells may serve as reference frames for place representations within that environment, determining the firing locations of grid cells in the MEC as well as of place cells in the hippocampus and spatially selective cells in other cortical regions (*20*) (SOM text).

References and Notes

1. J. O'Keefe, J. Dostrovsky, *Brain Res.* **34**, 171 (1971).
2. J. O'Keefe, L. Nadel, *The Hippocampus as a Cognitive Map* (Clarendon, Oxford, 1978).

3. E. I. Moser, E. Kropff, M.-B. Moser, *Annu. Rev. Neurosci.* **31**, 69 (2008).
4. J.B. Ranck Jr., in *Electrical Activity of the Archicortex*, G. Buzsáki, C. H. Vanderwolf, Eds. (Akademiai Kiado, Budapest, Hungary, 1985), pp. 217–220.
5. J. S. Taube, R. U. Muller, J. B. Ranck Jr., *J. Neurosci.* **10**, 420 (1990).
6. J. S. Taube, *Annu. Rev. Neurosci.* **30**, 181 (2007).
7. F. Sargolini *et al.*, *Science* **312**, 758 (2006).
8. M. Fyhn, S. Molden, M. P. Witter, E. I. Moser, M.-B. Moser, *Science* **305**, 1258 (2004).
9. T. Hafting, M. Fyhn, S. Molden, M.-B. Moser, E. I. Moser, *Nature* **436**, 801 (2005).
10. T. Hartley, N. Burgess, C. Lever, F. Cacucci, J. O'Keefe, *Hippocampus* **10**, 369 (2000).
11. C. Barry *et al.*, *Rev. Neurosci.* **17**, 71 (2006).
12. Materials and methods are available as supporting material on *Science* Online.
13. The proportion of border cells in the medial entorhinal cell population is overestimated because experiments were often not started on days with no known border cells in the cell sample. The estimates should be taken as an upper limit.
14. E. Bostock, R. U. Muller, J. L. Kubie, *Hippocampus* **1**, 193 (1991).
15. L. L. Colgin, E. I. Moser, M.-B. Moser, *Trends Neurosci.* **31**, 469 (2008).
16. M. Fyhn, T. Hafting, A. Treves, M.-B. Moser, E. I. Moser, *Nature* **446**, 190 (2007).
17. D. Yoganarasimha, X. Yu, J. J. Knierim, *J. Neurosci.* **26**, 622 (2006).
18. A small number of boundary-modulated cells has also been reported downstream of the hippocampus, in the subiculum (*11*), but whether these signals are derived from local neurons or from entorhinal axons [as in (*21*)] has not been established.
19. J. R. Whitlock, R. J. Sutherland, M. P. Witter, M.-B. Moser, E. I. Moser, *Proc. Natl. Acad. Sci. U.S.A.* **105**, 14755 (2008).
20. D. A. Nitz, *Neuron* **49**, 747 (2006).
21. J. K. Leutgeb, S. Leutgeb, M.-B. Moser, E. I. Moser, *Science* **315**, 961 (2007).
22. S. Leutgeb *et al.*, *Science* **309**, 619 (2005).
23. We thank N. Burgess and a number of other colleagues for helpful discussion and suggestions; M. P. Witter for advice about electrode location; M. Fyhn for donating an implanted animal; and A. M. Amundsgård, E. Sjulstad, I. M. F. Hammer, K. Haugen, K. Jenssen, R. Skjerpeng, H. Waade, and T. Åsmul for technical assistance. The work was supported by the Kavli Foundation, the Centre of Excellence scheme of the Norwegian Research Council, and a European Commission Framework 7 project (SPACEBRAIN).

Supporting Online Material

www.sciencemag.org/cgi/content/full/322/5909/1865/DC1
Materials and Methods
SOM Text
Figs. S1 to S12
References

26 September 2008; accepted 10 November 2008
10.1126/science.1166466

Representation of Geometric Borders in the Entorhinal Cortex

Trygve Solstad, Charlotte N. Boccara, Emilio Kropff, May-Britt Moser, and Edvard I. Moser

Science, **322** (5909), .
DOI: 10.1126/science.1166466